Research Report

Submitted To:
Dr. Dennis Collins (Investigator, Human Witness)
NTSB
September 22, 2007

A Preliminary Analysis of the Bridge 9340 Collapse at August 1st, 2007 and Some Suggestions

S. Hao Ph. D.
Advanced Analysis and Computing – Innovation and Invention (ACII)
347 Greenleaf, Wilmette, IL 60091
Tel: 8479209475; 8472742920
E-mail: hao0@suhao-acii.com
Web: www.suhao-acii.com

Sept. 22, 2007
(Based on the slides submitted to Dr. Dwight Forster, Deputy-Chief, Highway Section, NTSB at August 17, 2007)

Contents

Executive Summary

The research report was performed right after the collapse of bridge 9349. It contains four parts: computation-based structural and fracture analysis of the accident; reproduction of the failure process during the collapse; identification of the possible causes of the accident and suggestions of measurements to assist engineers for obtaining earlier prediction in future.

The study starts at the analysis of the defect-free 9340 bridge, understanding the original design and evaluating the possible safety issues. It has been concluded that the three-span steel bridge is a common design prototype in the past century. It uses the pilot spans at two ends to balance the load placed on the main span in middle, so as to achieve a long span distance with relatively light weight and low cost. By the enhanced deck-truss design with redundant diagonal main truss-reinforcements, the central part of the concrete deck in the main span, which is the location with the peak bending moment, is under relatively low compression load. However, from the viewpoint of the integrity analysis, this class of three-span bridges is essentially non-redundant in nature. When one span fails, other two spans can not survive, although the redundant trusses may keep local truss cell stable. Also a relative high tension stress (negative moment) appears on the upper trusses and deck part just above the supporting piers of the main span, which may promote fatigue growth of the defects around this area, especially at truss-joints. Nevertheless, since these drawbacks are so obvious, it is believed that they were carefully considered through corresponding high safety factor after original designer balanced all effective factors. The practical applications in past several decades prove that this class of design is conservative and thus safe in general if it is defect-free. Under this situation, computer simulation indicates that a structural failure will take place through the formation of plastic hinge at the middle part of main span, when the applied load reaches its plastic limit load that should be much higher than designed allowance.

Here we distinguish two concepts: the terminology “material’s failure” refers to the defects-induced localized material’s damage that may severely reduce the capacity of a single structural component against its load, whereas the terminology “structural failure” refers to the case when applied load reaches its limit load computed according to plasticity theory for steel bridge. The latter is usually obtained by bridge designer; on contrast, the former is usually beyond the consideration of conventional structural analysis based on, e.g. truss approximation.

According to this preliminary analysis and information on hands, a logic explanation of the 9340 bridge accident is a material’s failure induced structural failure. There are three evidences to support this preliminary conclusion: (i) The actual live load at the accident was within the window of the tolerance, although the average traffic flow constantly surpassed original estimate. (ii) Previous inspection did detect existing defects. (iii) The debris of wrecked bridge exhibits large scale damage and deformation in many truss members around the piers of main span; whereas a structural failure of beams/trusses network is usually characterized by the formation of localized plastic

hinges which induces kinematically permissible fields with the associated easily-large deformation; by which the plastic hinges accommodate the most deflection while other parts remains in the state of small deformation; in other word, staying at rigid or elastic.

As the applied load is believed within the design allowance, a consequent question will be: what is the driving force that triggered the rapid evolution of material's defect? This evolution reached its critical (bifurcation) point that caused structural instability after 40 years safety operation. Beyond the widely accepted speculation of the fatigue failure, the following three additional factors have been taken into account in this report: (a) the effects of slope, because the bridge descents about 7 feet from north to south end; (b) the rust-induced locking of the main span north-end's bearing-support, since additional geometrical constraint may lead to extremely high stresses; (c) the temperature changes induced intrinsic stress, which can be significant when all bearing-support turned into fixed-pin points, where the temperature fluctuation can be caused by daily and season's changes; the deicer fluid caused temperature difference between upper and lower truss members has also been taken into account.

In order to identify the actual failure model and find the cause, a series of two- and three-dimensional finite element computations have been conducted, in conjunction with damage models to simulate defects. The two-dimensional simplified model contains the main trusses members, focused on the dominant mechanisms; whereas the localized 3D finite element is used to check stress concentration around truss joint. Finally, the fully-scale model has been used for examining three-dimensional effects, verifying the dominant failure mode indicated by 2D analysis, and reproducing the actual process of the collapse.

For a long span of the structure like bridge 9340 the elastic deformation induced structural deflection can be significant; so in the computations the elastic-plastic material's model has been applied, instead of pure linear elasticity or rigid-perfect plasticity approximation. Additionally, a damage model has been implemented into the upper deck finite elements which allow the possible brittle facture at this part. This is because concrete is essentially "elastic" and "brittle" under tension, in spite of steel-bars' reinforcement. The deformation in concrete deck may not be sufficient to match the formation of plastic hinges in the upper level truss' members if no cracking and fracture. In reality a large-scale brittle fracture of concrete deck and the plastic collapse of nearby steel structure occur often simultaneously, since these two parts attach together and reinforce each other. Also, to simulate cracks and the corresponding crack propagation-induced steel truss/beam joints collapse, a cohesive model-based finite element has been pre-assigned to various suspicious locations in the computation, so as to reproduce the entire process of defects nucleation, fast propagation, localized material's failure and subsequent structure failure.

By varying initial locations of defects, boundary conditions (fixed-pin or roller-bearing pier support), and the fluctuation of temperatures, totally 21 cases of two-dimensional and 11 cases of three-dimensional computations have been carried out. The preliminary conclusion is that the bridge part above south eastern pier (pier 7 east) of

main span is the most possible spot with fatigue-induced defects, whereby the number one danger location is the upper level main truss joint and the second location is the truss joint near the pin point above the pier top. The analysis reveals that the rusted-induced bearing lock at the north end pier of main span can creates moderate uniaxial force but high bend moment in truss members over entire structure, which may induce significant high stress concentration around the joints near the supporting piers at two ends of the main span. This effect becomes critical when temperature fluctuates. By placing certain initial defects in the trusses joints near south end of main span while allowing brittle fracture in upper deck, the initial stage of the collapse, i.e. the failure of main span, has been reproduced numerically which quantitative matches the observed phenomena.

The analysis in this report concludes the existence of fatigue-induced defect before the accident. A more important task is probably to find the reasons that hamper us to have presentiments of the hiding risk that the bridge 9340 had. In order to avoid the similar tragedy happens again in the similar structured bridges on operation,

Based on the analysis and computations carried out and public available information, this report suggests a "hybrid bridge living-monitor system" to the veteran bridges that are suspected with defects and still under operation. This system including four parts: daily stress measurement by permanently-attached strain gauges (or other effective measurement methods) at key spots, regular inspection with shortened time interval and additional attentions to the key locations; thoroughly finite element analysis of the entire bridge structure including details of truss-joints, and the analysis of the existing risk based on the standards and the integrated information from both measurement and computations. This system should be able to provide dynamic information of the bridge's "health" so as to assist the corresponding administration make necessary decision on time. To make the system to be effective, this report suggests the attentions to the following three issues

- Bending moment in truss member and associated stress concentration: Accurate computation of the stress concentration around truss-joint is the prerequisite to obtain correct estimate of fatigue life. Due to the limited computation capability in past, it seems that the original design and subsequent early investigations could only treat the 9340 bridge as a truss-assembled structure, which led to the focus onto the forces and damage conditions in truss members. Although this is a commonly accepted engineering approach, in many cases it may underestimate the risk of fatigue-induced defect since it underestimates the bending moment induced stress in general, especially at truss-joints when rust-induced fixed-pin effect and thermal induced constraint become significant.
- The effect of stress superposition: strain gauges is an effective tool to capture and monitor "*in situ*" stresses on an engineering structure; however, it is limited to measure the change of stress after it is attached to the structure, for example, the difference of live loads between rush hours and that at midnight. A pre-existing stress state, such as residual stress and dead load (weight) induced stresses, can not be detected by strain gauge except it has been attached before the assembling of the bridge. Hence, merely strain gauge measurement [2] is usually insufficient

to obtain the actual stress amplitude of a bridge. An on site measurement in conjunction with computation is an efficient and accurate way to monitor stresses in an engineering structure, which is the central of the proposed "hybrid living-monitor system".

- Fatigue life estimate: The Miner's law is a recommended formula for estimate of the fatigue life of steel bridge; but it may underestimate the risk of the cases with existing macro-scale defect. This is because a fatigue-induced failure of steel components can be approximately divided into three stages: damages accumulation-induced macro-scale crack initiation, fatigue crack growth, and fast propagation with subsequent material's failure. Miner's law is originally developed to describe the first stage. The evolution speed of defect such as a crack growth is generally accelerated in the second stage when applied load remains. Paris' law is relatively accurate under this situation.

Also, regarding the ongoing investigation, this report suggests the following measurements:

- Preserve all broken sections, especially these near the pier-supports of the main span; the corresponding fractographic analysis may distinguish defects from different "ages". For example, a crack could be created before and during bridge component manufacturing and assembling, or was promoted by the fatigue loads in past 40 years, or occurred by ductile tearing and fast brittle crack propagation during the collapse, or is just the damages caused by the impact of fallen concrete deck.
- Perform microscale graphic analysis, such as TEM and SEM at certain positions; which may help to identify the deformation stage of the material and the stress level during the accident, which can be used to ascertain the occurrences of plastic hinges so as to verify computed failure model.
- Perform mechanical properties measurements by the specimens cut from failed component at key-positions, e.g. welded joint, heat effective zone, and steel matrix. These measurements include at least uniaxial tension, fracture toughness test and two classes of fatigue tests, i.e. the notched rotation bar test to measure the parameters in Miner's law and the fatigue crack propagation test in fracture mechanics specimen to measure the parameters of Paris' law.

The fundamental information provided by these suggested measurements will not only be useful to the current investigation, it could also be vital important for the safety evaluation of other similar-structured bridges under operation.

1. Introduction

On August 1st, 2007 the 1907 feet long three-span I-35W bridge (bridge 9340, see Fig.1) collapsed suddenly. As shown in Fig. 2, all three spanned bridge bodies fell into Mississippi River and its sides within seconds, caused dozen deaths and more injured. Before the occurrence of the disaster routine inspections did disclosure the existing defects such as cracks in various locations[1]; several safety assessment-based analyses had also been carried out to estimate the fatigue life of the bridge[2,3].

After mournfulness for the deaths and great regret to the suddenly disappearance of such a piece of engineering work in our daily life, the consequent questions are: what hampered us from foreboding the disaster in past and what an engineer can do to assist NTSB to find out the causes so as to prevent the tragedy happening again in future? All of these motivated the commitment of this research.

The conducted studies present in this report including three objectives: computation-based structural and fracture analysis of the bridge; reproduction of the failure process; and identification of the possible causes of the accident and the factors that might keep engineers from earlier prediction.

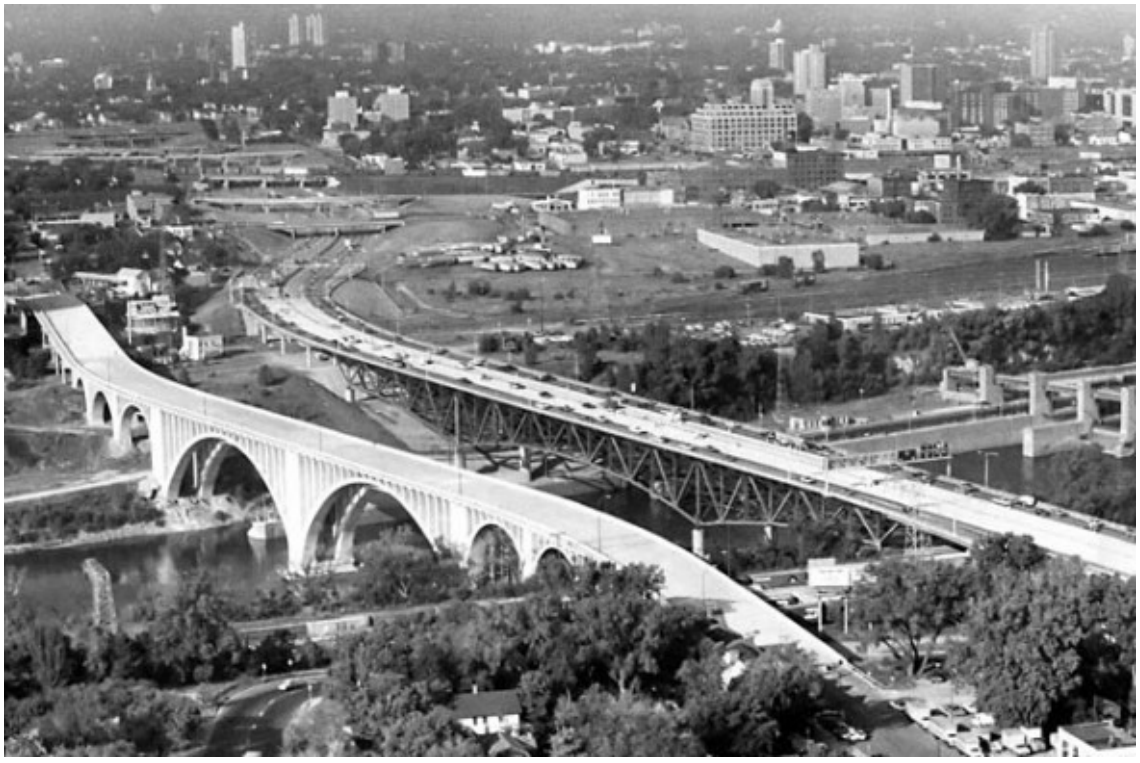

Fig. 1 The beautiful I-35W bridge 9340, Minneapolis, Minnesota.
(picture collected from twincity.com)

Fig. 2 Debris of the wrecked bridge 9340, after the collapse at August 1st, 2007.
(picture collected from Chicago Tribune)

2. Models and Approximations

2.1 Structural model

The bridge 9340 stretches from north to south over Mississippi River. It contains three structural parts: the main trusses (chords) that construct the frame of the bridge structure, the 108 feet wide steel-bar reinforced concrete deck with eight automobile tracks, and the sub-structured secondary truss-members that transfer the live-load on the upper concrete deck to the main truss-frame. It is reported that the bridge is equipped with anti-ice system, which pumps deicer fluid onto deck surface under appropriated temperature.

Fig. 3a is a copy of the original deck truss framing plan. Another side-view of the main truss frame is given by Fig. 3b, which demonstrated the descent upper deck design to match geographic environment. The major dimensions and sizes of the bridge are also marked in these two configurations. Fig. 3c is a sketch of the substructure of the secondary truss members. The Figures 3a,b,c are collected from [1,2]. As illustrated in Fig. 4, the truss spans have a fixed bearing (pin point) at pier 7 and three roller bearings in piers 5, 6, and 8, respectively.

As a convention in this analysis, a right-hand Cartesian coordinate has been defined, originated at the pier 5 in Fig. 4 - near the north most end of the bridge. So the x-coordinate axis horizontally points to the south whereas the z axis points to west and the y axis points onto sky. As illustrated in Fig. 3a and Fig. 4, the capital letters U_n and L_n with the index n denote the upper and low joints of main truss members, respectively,

on the north half of the bridge while $U_n^{'}$, $L_n^{'}$ denote the joints on the south half. In three-dimensional presentation, the subscripts "*E*" and "*W*" are used to indicate the objects in East side and West side, respectively; e.g. $Pier7_W$, U_{3E}, and so on. Hence, each main truss member can be denoted by the symbols of the joints at its two ends; for example, the right-most upper level truss in Fig. 4 can be denoted as $U_1^{'}U_0^{'}$.

2.2 The Challenges

Although the structure of bridge 9340 is relatively simple according to today's technical standard, to obtain accurate analysis is still very challenging due to the sophistications in its design, manufacturing, and long operation history. The main complexities can be listed as below:

(i) Pre-stress state in concrete slabs and residual stresses in steel components created during welding and assembling are unknown.

(ii) According to the inspection report [1] the conditions of roller bearings at piers 6 and 7 are poor; since they are the supporting points of main truss span, a lock at pier 6 can lead to remarkable high geometric constraint and associated stresses.

(iii) The daily and season's temperature change are relatively significant, which may introduce considerable high thermal stress, especially when the roller bearing at pier 6 is locked due to rust and surface damage.

(iv) The winter's daily deicer-operation creates the temperature difference between upper and lower truss members, which may also induce additional thermal stresses.

(v) The descent deck surface design makes the bridge structure become unsymmetrical.

(vi) No quantitative information about the welding process, residual stresses, and corrosion/rust-induced damages in the structure.

(vii) The bridge is under a combination of dead-load (weight), live-load (traffics and wind), and uncertain thermal loads.

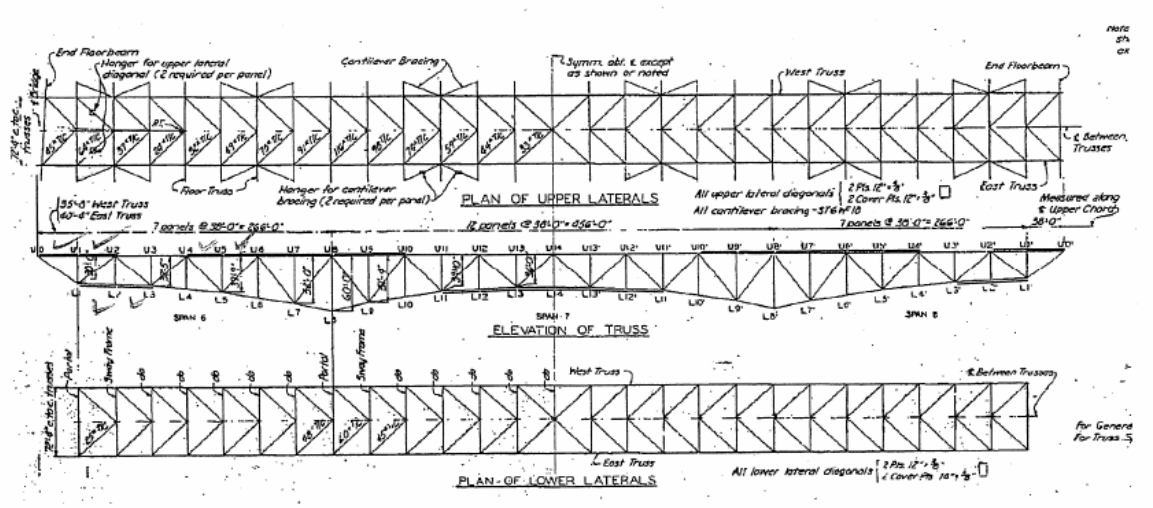

(a) Deck Truss Framing Plan from original contract plan

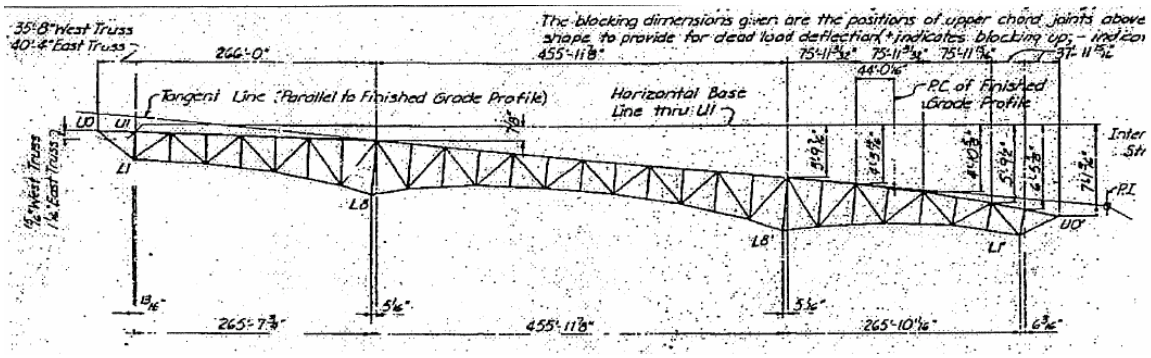

(b) truss layout

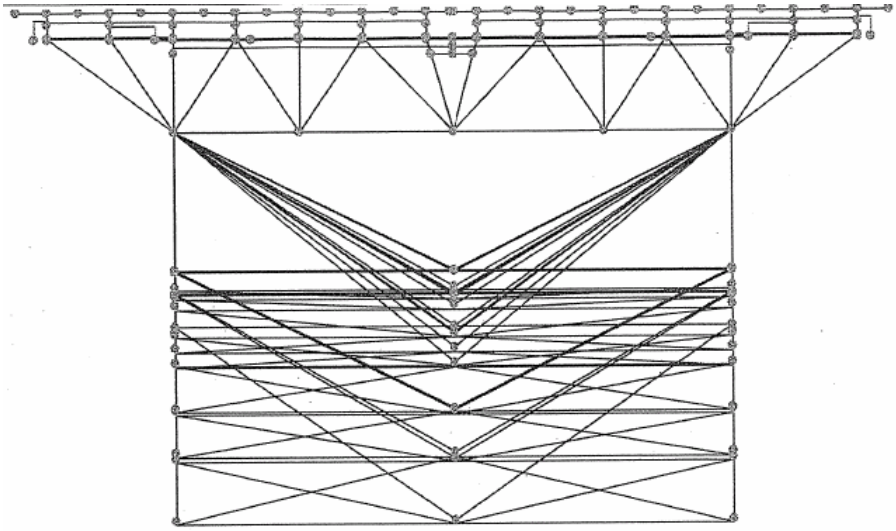

(c) substructure of secondary truss members

Fig. 3 The superstructure of desk truss frame (a,b) and the substructure of secondary trusses (c) [1]

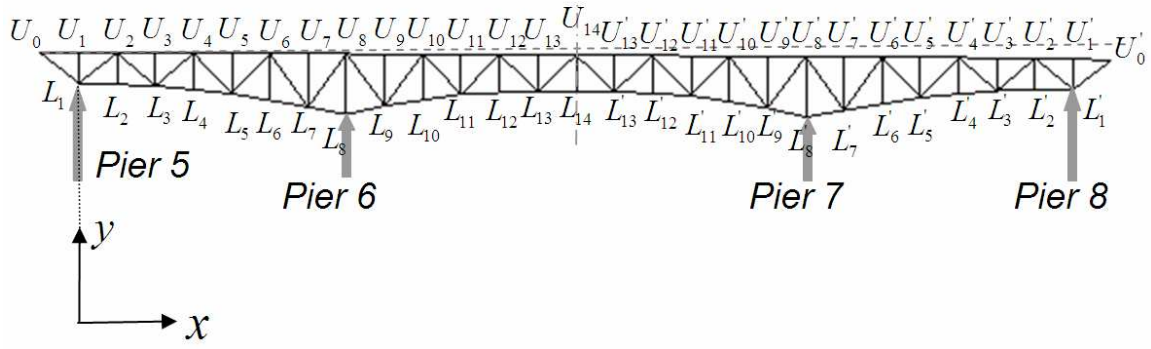

Fig. 4 Coordinates, conventional notations of the main truss members, and support piers.

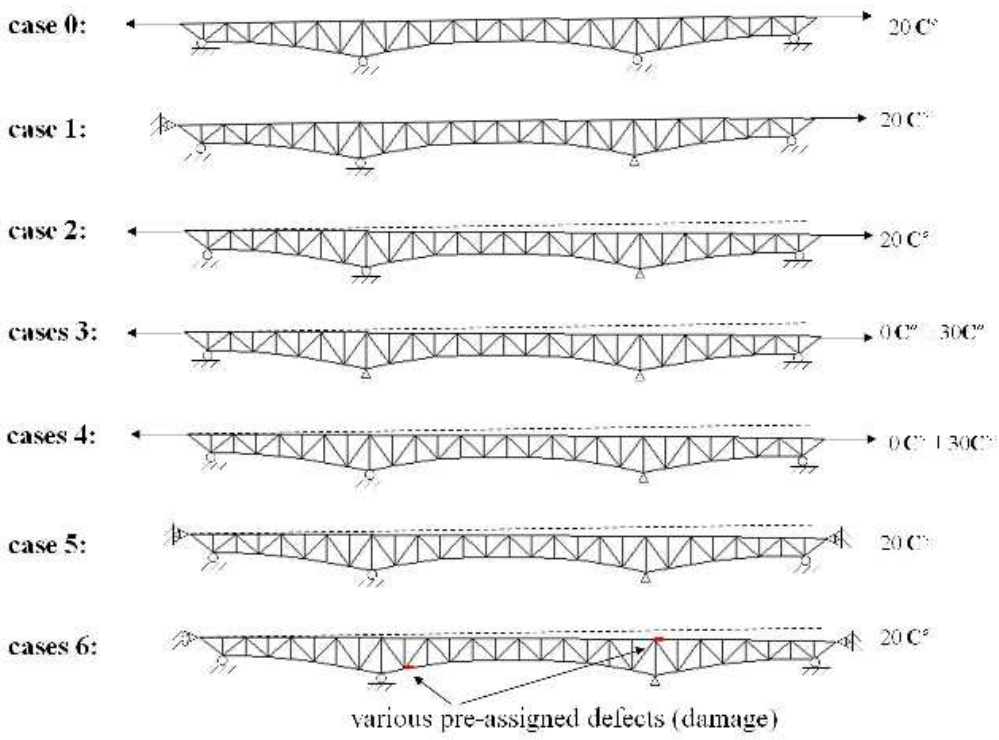

Fig. 5a Cases analyzed

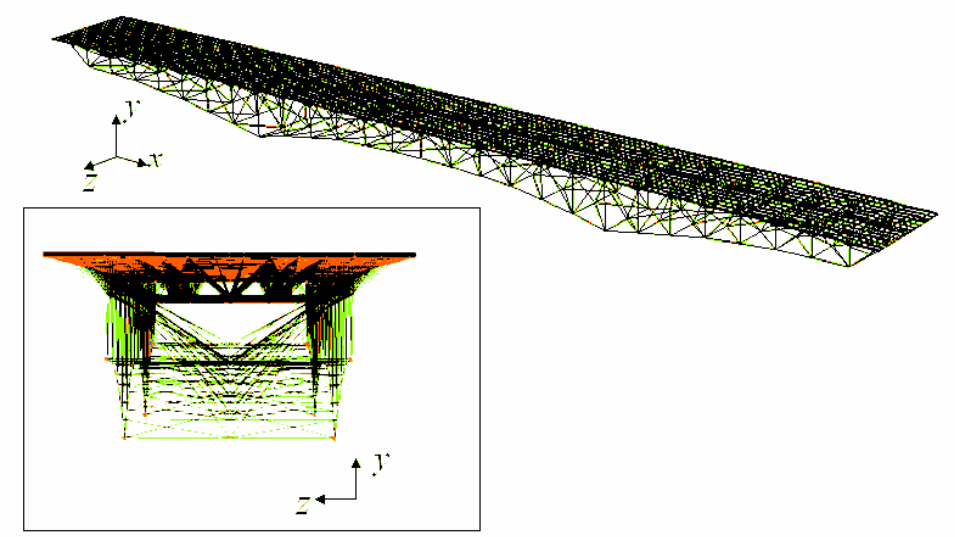

Fig. 5b The 3D Finite Element Model

2.3 Cases Analyzed

In order to assist NTBC to explore the mechanisms that caused the accident while clarify disclosed safety issues in other bridges with the similar structures, in this report a set of two- and three-dimensional finite element structural models have been developed, in conjunction with a damage-induced fracture model and a cohesive model for material's failure analysis. Except the wind-load, the complexities (i) to (vii) listed above have been taken into account through the simplifications categorized by the seven basic cases

plotted in Fig. 5a, whereby the environment factor(temperature change), bearing conditions and pre-existing defects have been transferred into mechanical boundary conditions, loading conditions, and pre-assigned damage zones. The correspondent case by case studies will be performed in the following sections. Plotted in Fig. 5b are the two views of the developed three-dimensional finite element model.

2.4 Cohesive Model and Damage Material's Model

To effectively reproduce the phenomena of damage-induced material's failure and macro-scale defect propagation-induced structural failure, in the cases 6 of the Fig. 5a a damage material's constitutive model (stress-strain relation) and a cohesive model have been implemented into numerical computations. The physical meanings of these two models are illustrated in Fig. 6; which can be briefly explained as following:

Starting from the left side of the figure, the left-upper corner is a defect-free plate under uniaxial tension; the corresponding average stress-strain curve is illustrated by the ascended solid line started from origin and the connected thick long-dash line denoted by $a = 0$ in the diagram in the middle, showing a regular strain hardening behavior; where the "average strain" means the elongation of the plate divided by its original length while the "average stress" is the applied load divided by the plate section area without crack. When a crack presents in the plate, as plotted on the left-lower corner, the correspondent average stress-strain relations in the middle graph is a group of thin short-dashed lines corresponding to different initial crack lengths when no propagation occurs. However, when the crack does grow, e.g. from a_0 to a_2, accordingly the average stress-strain curve is the solid line connected by the dots, demonstrating the trend of elastic-loading and strain softening in average. When crack tip reaches the right side of the specimen, this strain softening brings stress to zero since the plate structure totally loses the capacity against applied load.

Considering crack growth is the separation of two material's surfaces, the above mentioned process of crack growth/average strain softening can be phenomenologically modeled by the nonlinear springs attached to the opposite material's surfaces; these springs are obeying the same softening law, as illustrated in the box on the right-lower corner. Such a model is conventionally termed "cohesive model".

On other hand, this material's separation is actually an accumulation of the microscale damage evolution, for example, the nucleation, growth, and coalescence of microcracks and cavities. The phenomenon of damage evolution can also be directly embedded into material's constitutive law through certain mathematic expression to link the averaged strength to the amplitude of damages at each material's element. Under this approximation, a crack propagation eventually becomes the extension of a strip zone with damage concentration, as illustrated by the plot in the right-upper corner box.

In the computations performed in this report the damage accumulation model has been employed as the constitutive law to describe the stress-strain response and fracture behavior of concrete deck. The cohesive law has been implemented into concrete and

steel members at key-positions to promote formation of plastic hinges and to represent the evolution of existing defects. The difference in initial defect's size and between plastic hinge and crack propagation are represented by adjusting the cohesive model and damage parameters in computations

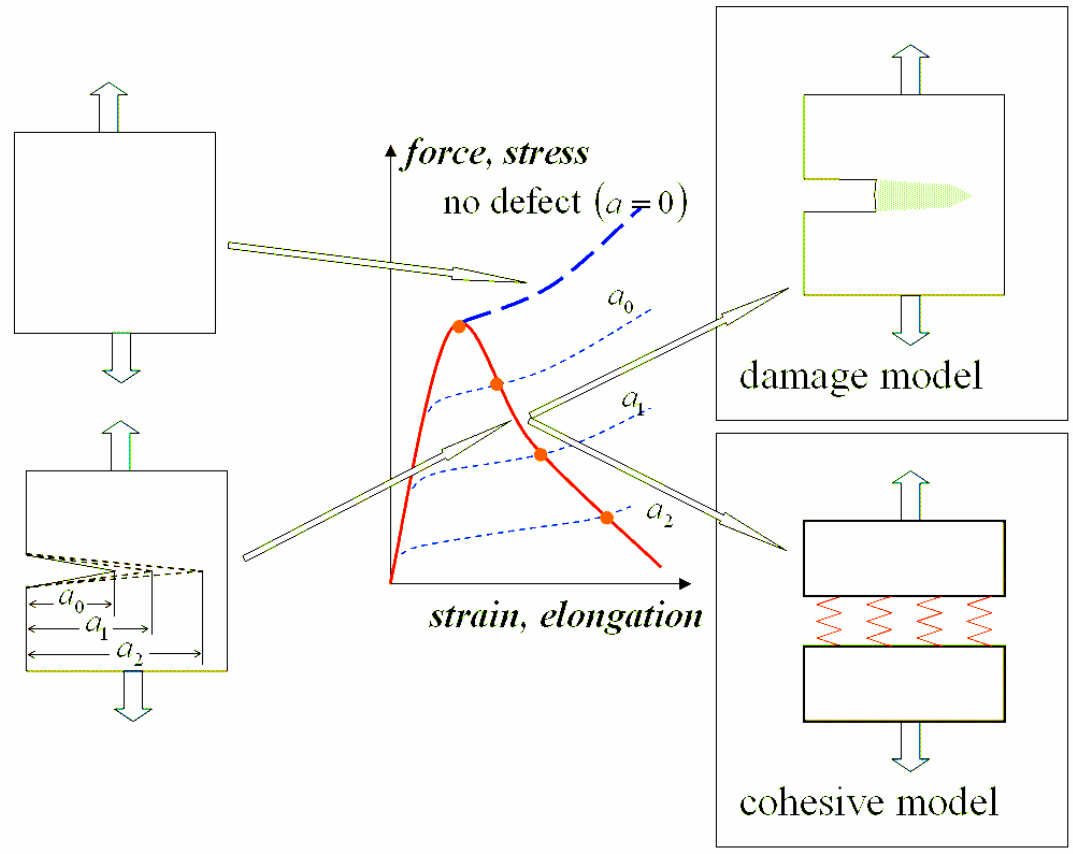

Fig. 6 Damage-Induced Crack Growth Model and Nonlinear-Spring Cohesive Model (Needleman, Rice); the fundament information about fracture mechanics can be found, e.g. in Advanced Fracture Mechanics, v.2, editor Leibowitz.

2.5 Approximations

In the finite element computations of this report the following approximations have been applied:

(1) All piers are placed on fixed solid basis, no sunk or deflection on any pier support point.
(2) The loading process is divided into two steps for the analysis under constant temperature; the first step imposes dead-load (weight), followed by gradually increasing live-load on the concrete deck. This process is divided into three steps when temperature fluctuation is taken into account, by which an additional step in-between has been inserted for temperature-induced load.
(3) The live-load is presumed uniformly distributed over the deck surface.
(4) Quasi-static analysis, the effect of inertia is omitted.
(5) Wind-load is not counted.

(6) Both concrete deck and steel members are obeying elastic-plastic stress-strain laws. The materials' and geometric parameters are picked up from literatures; hence quantitative difference from the accurate analysis may exist.

3 Case by Case Studies

3.1 Defect-Free 9340 Bridge (Cases 0, 1, 2, 5)

The study starts at the defect-free 9340 bridge, understanding the original design and evaluating the possible safety issues.

By reviewing the design history of bridges in past century, one may find that the structure of 9340 was a widely-used common prototype. The central idea of this design is to pursue the longest main span with minimum cost. By utilizing the pilot spans at two ends to balance the load on main span, the design effectively reduced the maximum bending moment at the center of the main span to the level about half of the single span structure, as illustrated by the theoretical solutions of the simplified straight beams in Fig. 7. The deck truss design of 9340 also makes the concrete deck is under compression stress at the center of the bridge, where the maximum bending moment occurs. However, as a trade-off, a negative moment appears at the main span's ending support points. For a 1:2:1 length ratio three-span structure, the simplified solution of Fig. 7 indicates the ratio between the moment at the ending support points and the peak moment at the center is about 5/4.

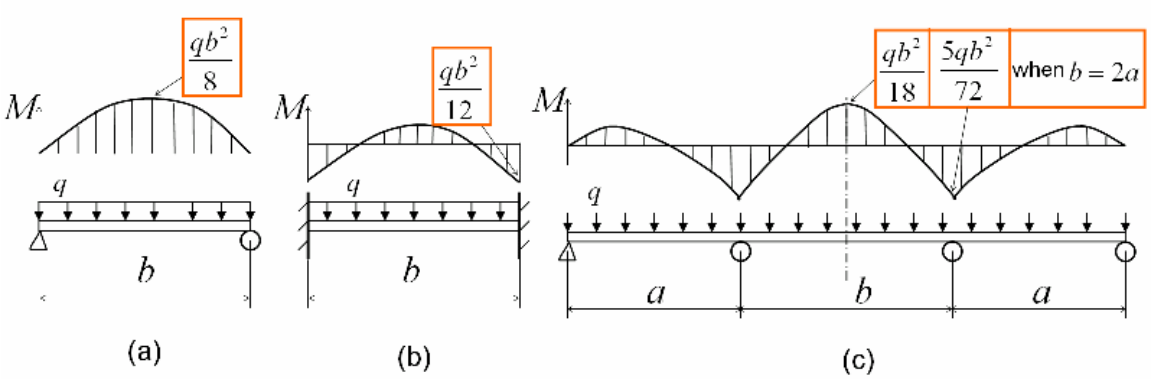

Fig. 7 A simplified model of straight beam under uniformly distributed load for demonstrating the idea of three-span bridge design in 9340: as compared to the single span structures (a,b), the peak bending moment of (c) is about 80% lower than (a) and 20% lower than (b).

From the viewpoint of integrity analysis, this three-span structure is essentially non-redundant in nature. When one span fails, load condition on other two spans will transfer back to the situation similar to the case (a) in Fig.7; so they can not survive, although the additional diagonal redundant trusses reinforce each individual truss cell to be stable. Also a relative high tension stress appears on the upper main trusses just above the piers of main span. Nevertheless, as these drawbacks are so obvious, it is believed that they had been carefully considered through additional high safety factor after original

designer balanced all effective factors. The practical operation in past several decades proves this class of design being conservative and safe in general, when no macroscale defect presents.

The three-span beam model (c) in Fig. 7 is quiet similar to the case0. Plotted in Fig. 8a are the computed uniaxial forces on each main truss members when the live-load reaches the level of 10% its plastic limit, where the forces on diagonal truss members are their absolute values. The result in this plot demonstrates two locations with maximum uniaxial stress: the middle section with the peak tension at lower level truss and compression at upper level truss, and the sections above the main span supporting points with the inverse distribution. The second location is the weakest link of the bridge because the high tension may result in high stress concentration at trusses joint; the tension stress will also be transferred into brittle concrete deck. This location will get more attention in the following analysis.

In Fig. 8a one may notice that a positive (tension) force appears in the vertical main truss member, which caused by dead-load (weight) since the live-load on the upper deck is low. Fig. 8b is the distributions of bending moment, where the upper, diagonal and lower main truss members present a similar trend. In both Figs. 8a and 8b, the case 3c basically coincides the distribution of case 3b.

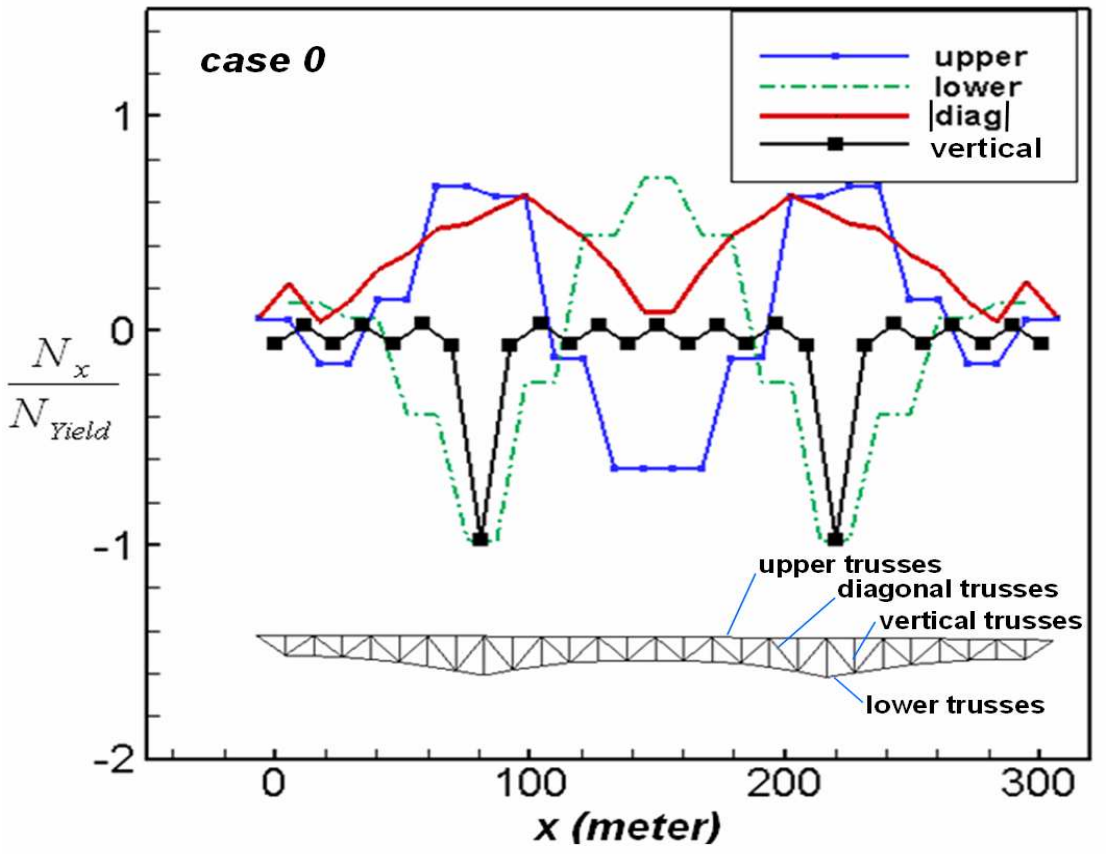

Fig. 8a Computed force of the truss members at different locations, where N_x is the uniaxial force in each truss and N_{Yield} is the maximum N_x when the structure starts yield.

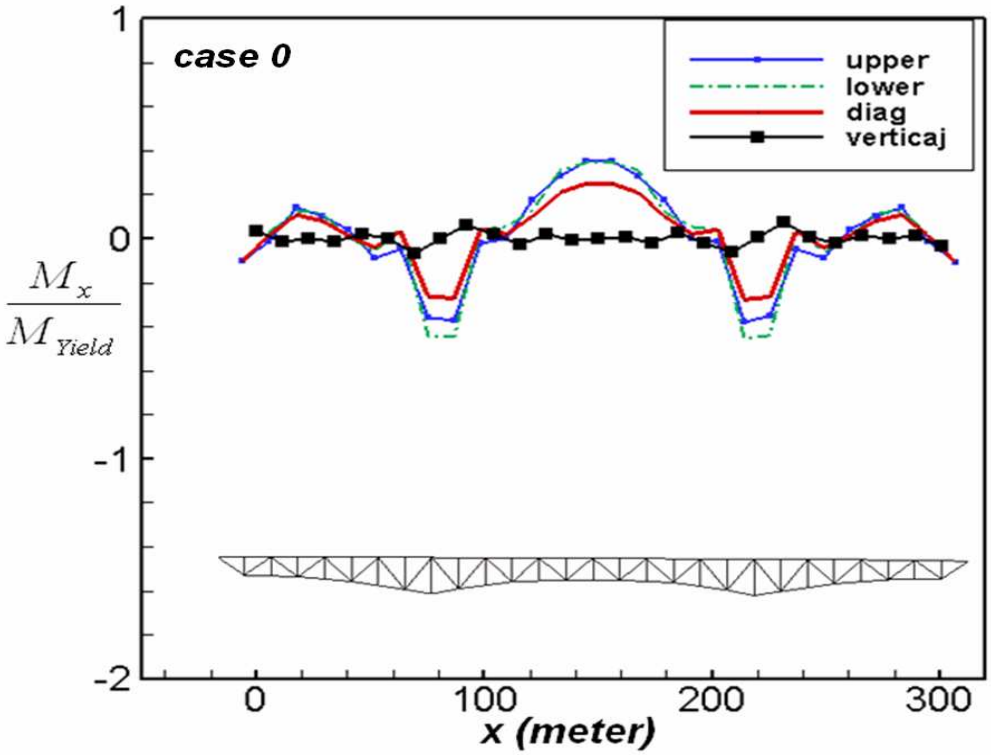

Fig. 8b Computed bending moment in the truss members at different location, where M_{Yield} is the moment when the structural starts yield.

Plotted in Fig. 9a are the uniaxial force on the upper level truss for the cases 0, 1, 2, and 5, where case 2 is the actual design with the surface deck descent to south with fixed-pin support at the main span's south end. One finds that the tension force distribution of case 2 is the same as that in the simplest case0, which means the fixed pin-point boundary condition at pier 7 trades off the effect of descent of the surface deck. This reflects the sophisticated consideration of the original designer.

By increasing the horizontal forces imposed on the both ends of the bridge in case 2, it will eventually reaches the state prescribed by the case 5. The corresponding tension force in upper main truss members is also plotted in Fig. 9a, by which one can find that the case5 is essentially same as case2 but with another amplitude of horizontal force at south end.

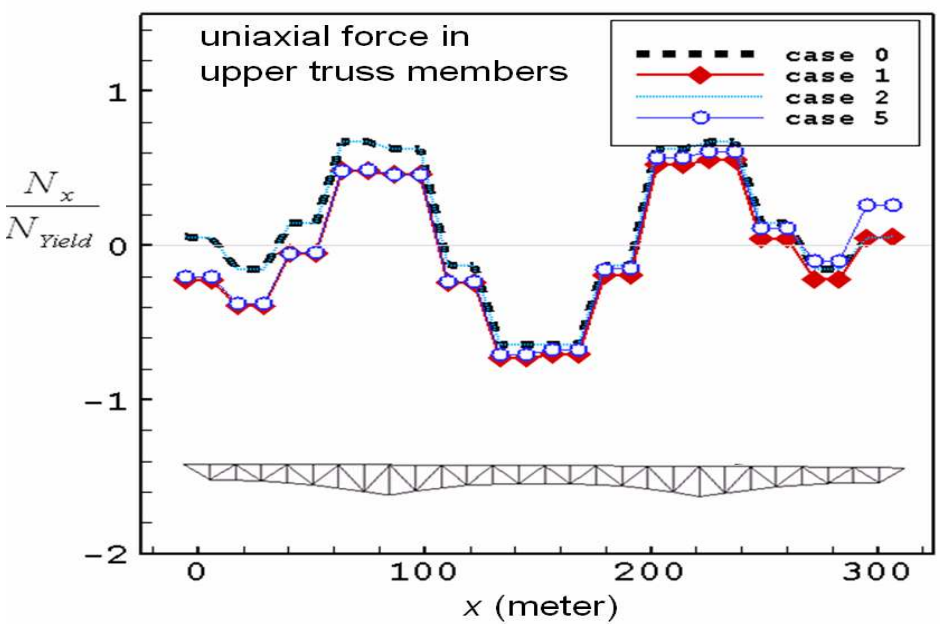

Fig. 9a The distributions of uniaxial force in the upper truss members for cases0,1,2,5; where the curves of case 2 and case 0 coincide each other whereas the case 1 matches case 5 in almost entire length but with slight difference on south end (right).

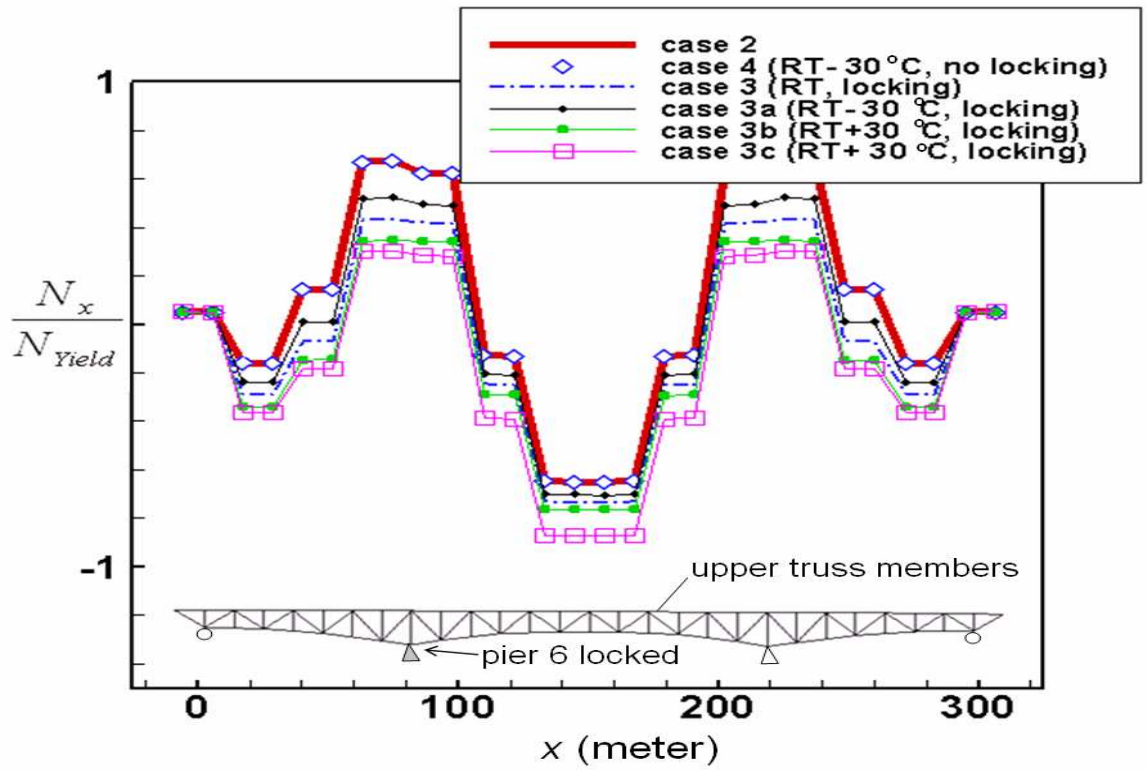

Fig. 9b The distributions of tension force in upper truss members for the cases with roller bearing-lock or thermal stresses, where "RT" stands for room temperature; "locking" means the lock of roller bearing at pier 6; case 3c refers to thermal-induced load when temperature rises at upper truss-members while no change in other parts

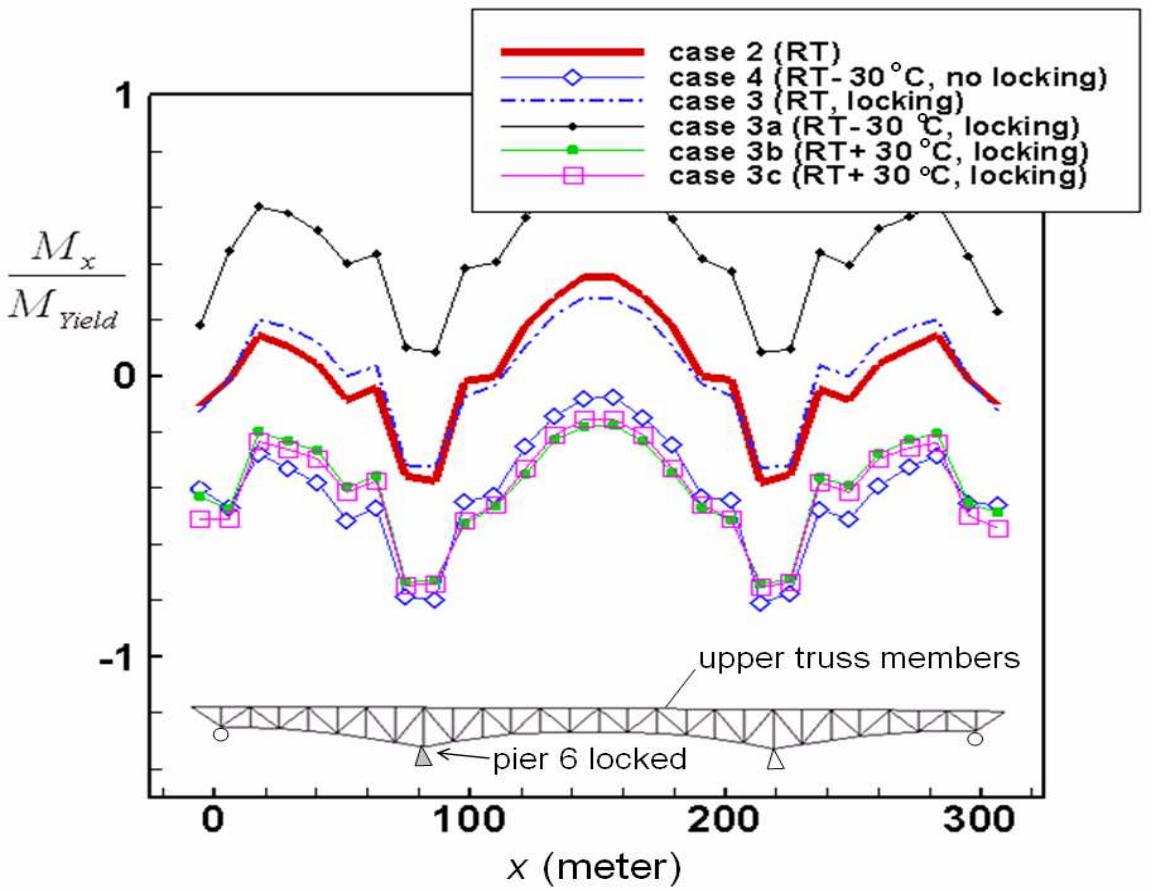

Fig. 9c: The distributions of bending moment in upper truss members for the cases with roller bearing-lock or temperature changes; significant effects can been seen. In this figure "RT" stands for room temperature; "locking" means the lock of roller bearing at pier 6; the case 3c refers to thermal-induced load when temperature rises at upper truss-members while no change in other parts

3.2 Cases 3 and 4: Effects of the Roller Bearing-Lock and Temperature Changes

The earlier inspection report indicates the roller bearing condition at pier 5 and 8 is acceptable, but the condition at pier 6 is poor due to rust and corrosion. When this roller is fully locked, it becomes a fixed pin point so the bridge can be modeled by the case 3. Fig. 9b are the distributions of axial force in upper main truss members under the following conditions: (i)case2; (ii)case4, no roller-locking but temperature changes; (iii)case3, with roller-locking but no temperature change; (iv)case3a and case3b, with both roller-locking and temperature changes. (v)case3c, with both roller-locking but only the upper lever truss members suffer the temperature change; In cases 4 and 3a,b the temperature vary from 0 to ± 30 ^{o}C over entire bridge and for case 3c just over the upper deck surface. These results shows that the roller-locking and temperature change have moderate effects on the uniaxial force. The locked roller at pier 6 causes compression force on the upper level trusses in general (case 3). When temperature rises, an additional compression force will be added; whereas a tension force is created when temperature drops. These temperature-induced changes of the uniaxial force are due to the constraint

of the fixed pin-points. Its amplitude is relatively small as compared with that caused by dead+live-load. One can find that the case2 and case4 coincides each other, implying that locking is the prerequisite to uniaxial thermal stress.

However, when we look at the bending moments plotted in Fig. 9c, a totally different phenomenon appears: severe high moments present in both the locations near pin-points and central. This time the case2 and case3 coincides each other, indicating the dominance of temperature changes.

It is the common knowledge that for, e.g., a square-sectioned truss or beam with area S and height $2h$, under elastic condition the maximum stress $\sigma_{\max}$ is the sum of uniaxial stress and the product of the bending moment M and half of the section height h then divided section module I:

$$\sigma_{\max} = \frac{N_x}{S} \pm \frac{Mh}{I} \tag{1}$$

where N_x is uniaxial force in truss and S is the section area. When steel yields, assuming perfectly-plasticity, a plastic hinge will be formed, the corresponding stress will reduce to:

$$\sigma_{\max} = \frac{N_x}{S} \pm \frac{4M}{h^2} = \frac{N_x}{S} \pm \sigma_Y \tag{2}$$

where σ_Y is the yield strength of the material.

The relations (1,2) indicate bending moment induces remarkable stress. Under certain condition, e.g. at the truss joints U_8' in Fig. 4, the addition material's constraint may prohibit the formation of plastic hinge and result in high stress concentration.

Thus, one can conclude that the locked roller, in conjunction with temperature changes, will create significant high stress concentration at the upper level, which may significantly accelerate the nucleation and fatigue growth of defects.

4 Failure Analysis of the Accident

Here we first distinguish two concepts: the terminology "material's failure" refers to the defects-induced localized material's damage that may severely reduce the capacity of a single structural component against its load, whereas the terminology "structural failure" refers to the case when applied load reaches its limit load computed according to plasticity theory for steel bridge. The latter is usually obtained by bridge designer; on contrast, the former is usually beyond the consideration of conventional structural analysis based on, e.g. truss approximation.

4.1 The Pattern of Structural Failure (Case 2)

Direct observations disclosed to public indicate that the accident occurred through at least two stages: (1) the collapses of main span and the south pilot span; (2) the collapse of the north pilot span. In this analysis we focus on the initial stage.

For a defect-free steel bridge, a structural failure will take place when the applied load reaches its limit load calculated according to rigid-perfectly-plastic theory. Localized structural buckling may reduce the limit load. The computer simulation performed in this study indicates that the structural failure for 9340 begins with the formation of plastic hinge at the middle part of main span, as demonstrated by Fig. 10. This figure contains a snap-shot of the large deformation process during the failure of the case 6a. From this figure one can find the secondary plastic hinge near the two main span's support points. The locations of these plastic hinges match the locations with peak stress plotted in Fig. 8a.

By comparing the failure pattern in Fig. 10 with the debris of the wrecked bridge in Fig. 2, it looks like that the collapse of 9340 bridge is triggered by defects-induced material's failure at several locations that do not necessarily match the plastic hinges showing off in the structural failure in Fig. 10a. These distributed material's failure sites severely reduced the capacity of the bridge against its load and, leading to subsequent structural failure with different mode. There are three evidences to support this conclusion: (i) The actual live load at the accident was within the window of the tolerance [2], although the average traffic flow constantly surpassed original estimate. (ii) Previous inspection did detect existing defects. (iii) The preliminary observation, e.g. Fig. 2, shows that the distributed debris exhibit large scale damage and deformation in many truss members around the piers of main span, instead of concentration to certain localized plastic hinges.

4.2 Material's Failure Induced Structural Failure

Supposing that material's failure does cause the collapse, consequently the key-issues are to identify the location and size of pre-existing defect(s). Due to limited information, in this report the damage constitutive model is implemented into concrete deck and the cohesive model has been pre-assigned to several suspected locations to represent possible existing defects. The size of each defect is modeled by adjusting the strength and softening rate of cohesive law.

Although Figs. 8-9 predict the areas with stress peaks, question remains about the exact location of the pre-existing defect. In order to find the most possible location, three-dimensional computations of the beam(truss)-joint model presented in Fig. 11a have conducted, instead of the approximations such truss or beam that is adopted in the 3D analysis of Fig. 5b and 10. The finite element meshes and results are briefly outlined in Fig. 11b, where two cases: the uniaxial force dominants in bottom beam and the bending moment dominants have been computed. According to the contours of Von-Mises stress (equivalent) a strong stress concentration appears in the latter. On other hand, Fig. 8b and 9c indicate the remarkable bending moment, especially pier 6 is locked and temperature fluctuation occurs. Since fatigue crack initiation and growth are very sensitive to stress

concentration such as that presented in the bending case of Fig. 11b, this report focuses on the cases of defects at truss(beam)-joint.

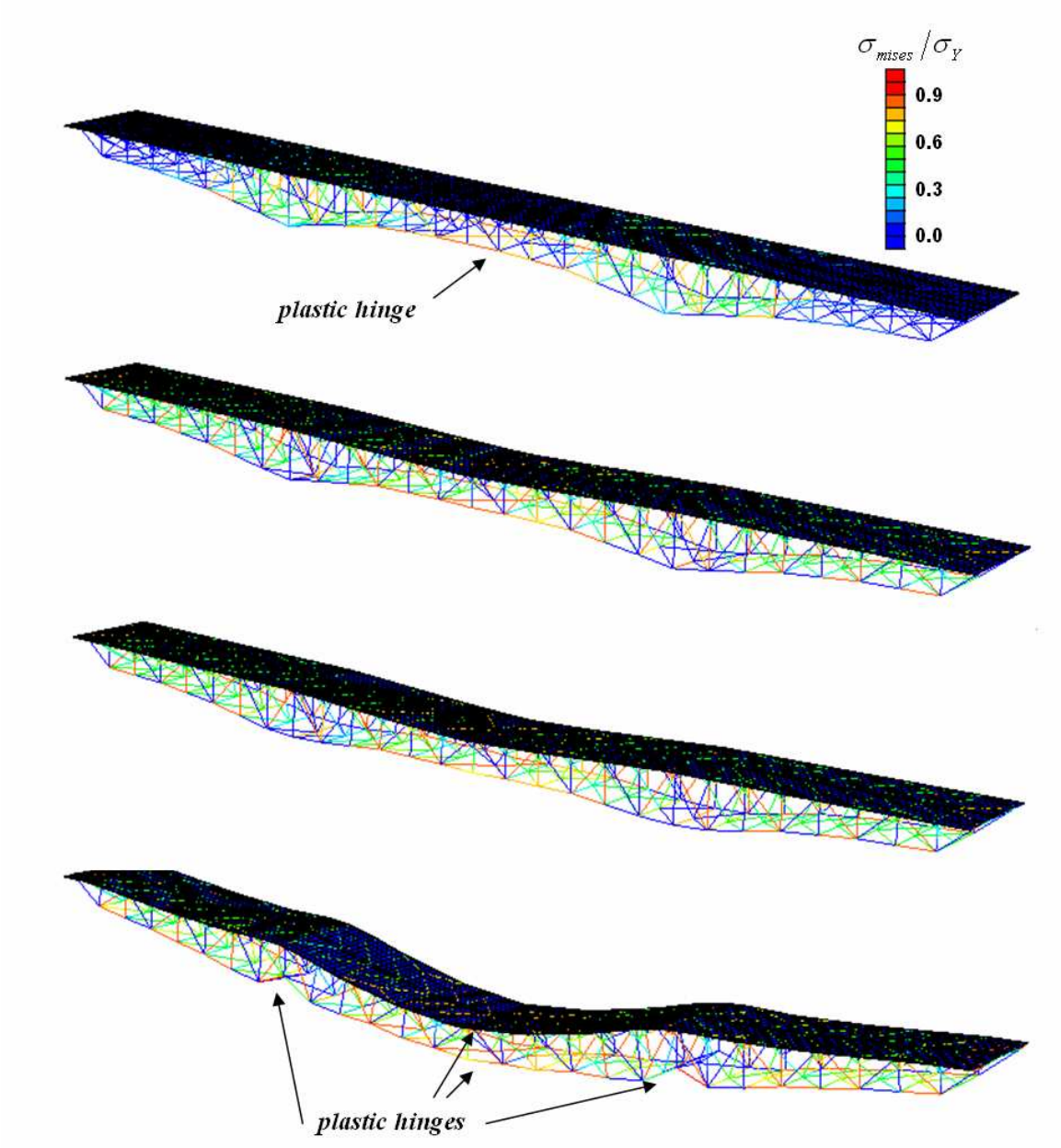

Fig. 10 A snap-shot of the process of structural failure.

According the analysis in the previously and released inspection reports, the following locations are supposed to be the suspected spots of defects, hence, the most dangerous sites to induce subsequent material's failure:

Case 6a: The far-south or north end around $U_0^{'}$ or U_0 in Fig. 4; where fatigue crack has been detected before.

Case 6b: The middle point of the lower main trusses, i.e. L_{14} and its surrounding, where the maximum tension takes place, as indicated by Fig. 8a

Case 6c: The upper truss joints and deck above the main supporting points, i.e. the areas around $U_6^{'} - U_{10}^{'}$ and $U_6 - U_{10}$.

Case 6d: The main trusses near the two main supporting points $U_8^{'}$ and U_8.

Case 6e: The combination of Case 6c and 6d.

In the computations of the cases listed above, the boundary and load conditions of case 2 are applied.

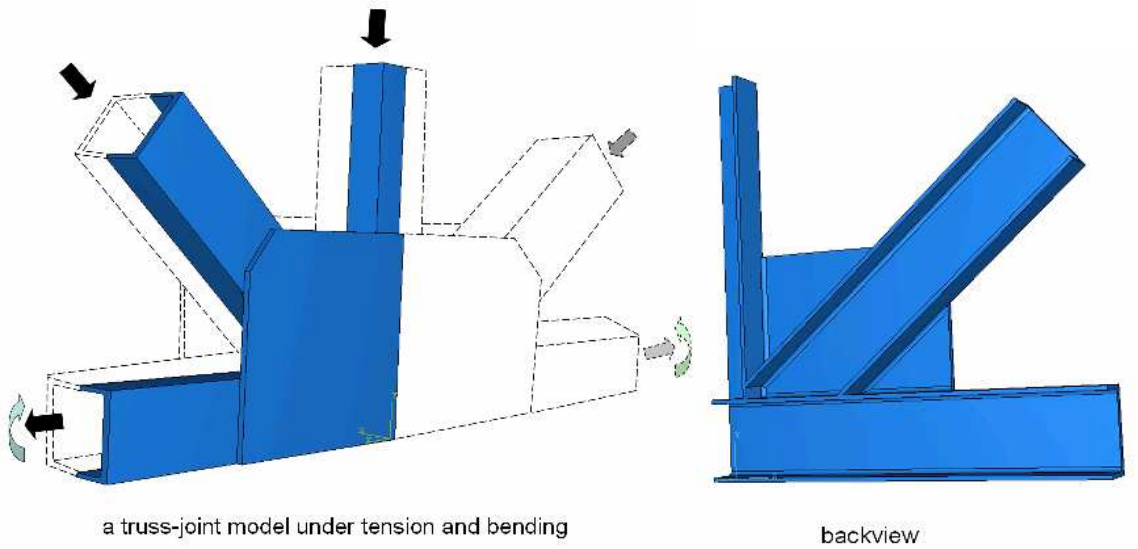

Fig. 11a 3D truss(beam)-joint model; due to the symmetry only a quarter of the structure is analyzed

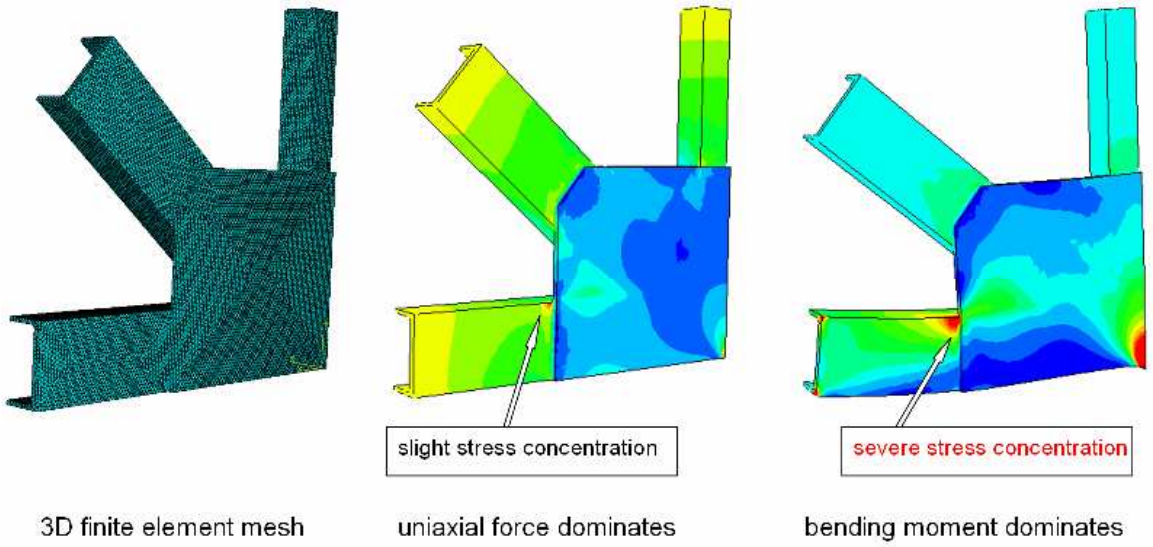

Fig. 11b Finite element mesh and contours of equivalent stress (Von Mises) for the case of uniaxial force dominants and bending moment dominants in the bottom beam; a strong stress concentration appear in the latter case, which usually triggers fatigue crack.

Cases 6a, 6b

As illustrated by Fig. 12a, the deformation fields of case 6a and 6b exhibit the similar pattern as that in structural failure. In case 6b the defect at the joint L_{14} is identical to an earlier developed plastic hinge. The fracture at this joint causes the plastic hinges around U_{14} in upper truss. It basically cased "folding" of main span since its middle point is able to accommodate more rotation, which also reduces the moment at its ends. Similarly, considering the extreme situation of case 6a that no horizontal force or displacement constraint is imposed on the two ends of the bridge, the middle part of main span will sink easily after plastic hinge formation when the roller bearing on pier 5, 6, and 8 work. That is why no significant plastic hinge formation near the supporting points.

A common feature for both the cases is that the main span folds after its central point becomes a "plastic hinge". However, the information provided by video type and eyewitness and aired by mediums emphasized that the main span started breaking at the two ends, then the body fell into water horizontally, which excludes case 6a and 6b from further consideration.

Cases 6c, 6d, 6e

Fig. 12b shows the computations with highlighted different initial defect's location. A character in common for all of these examples is that, once a defect becomes active, it leads to new pattern of structural failure, as explained by the simplified straight beam model depicted in Fig. 13. In this model an active defect around the pin-point near right end actually transfers this fixed pin into a flexible support, shifting the moment distribution to the left half of the beam. The computed moment and uniaxial force are plotted in Fig. 14. An extreme situation is that the pin-point loses the capacity against

load entirely, so the main and right pilot spans become a single span, as depicted by Fig. 13.

Hence, the cases 6c,d,e are more dangerous than others in general for the integrity of the structure. This is because in these cases defects present at the locations with the highest stresses, where the rusty-induced bearing-lock and temperature changes will amplify the stress concentration significantly. This concentration brings up high driving force that accelerates the propagation of the defects, which ultimately leads to the localized material's failure with the subsequent final structural failure.

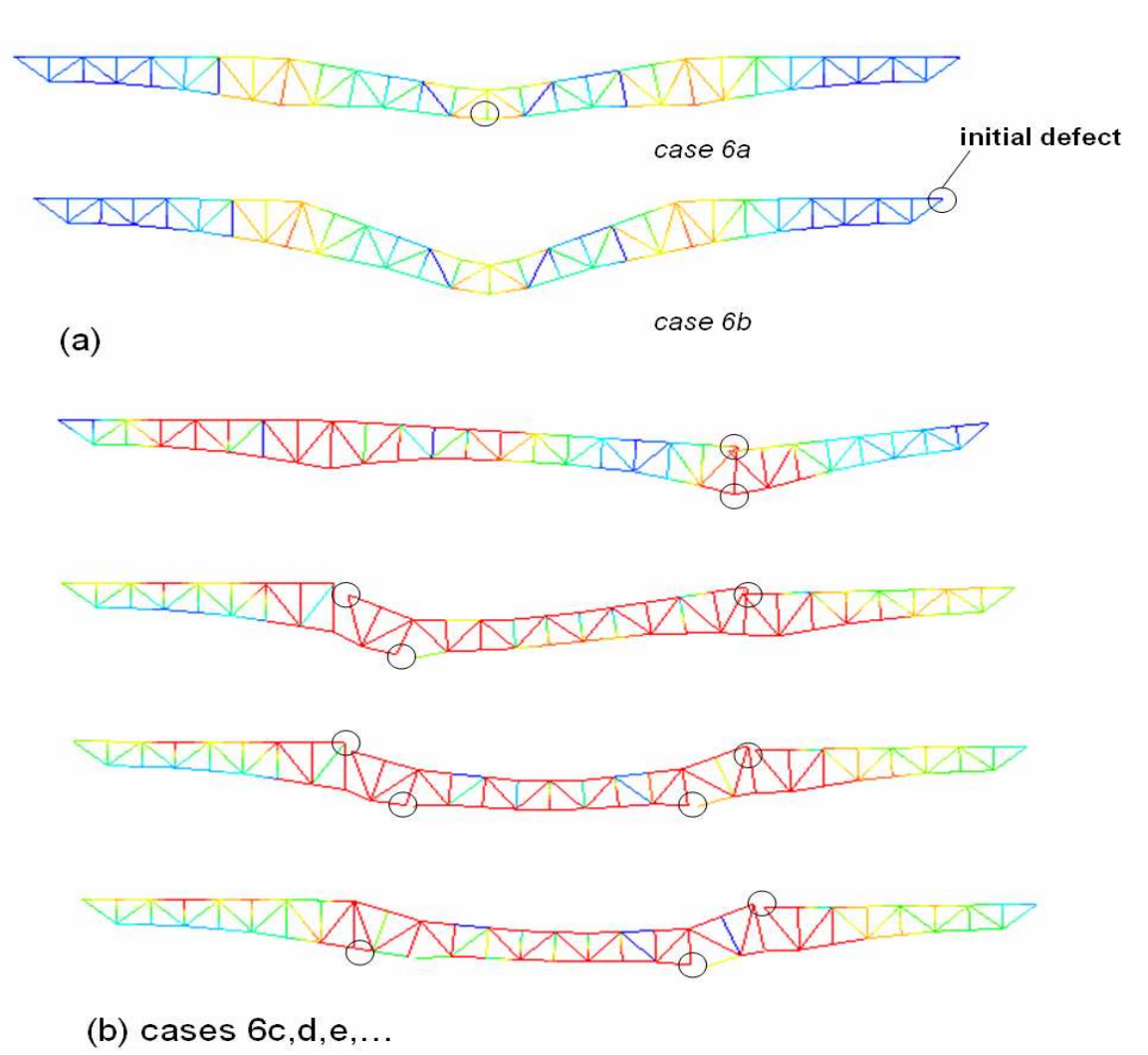

Fig. 12 The patterns of structural failure caused by the material's failure with pre-assigned defects

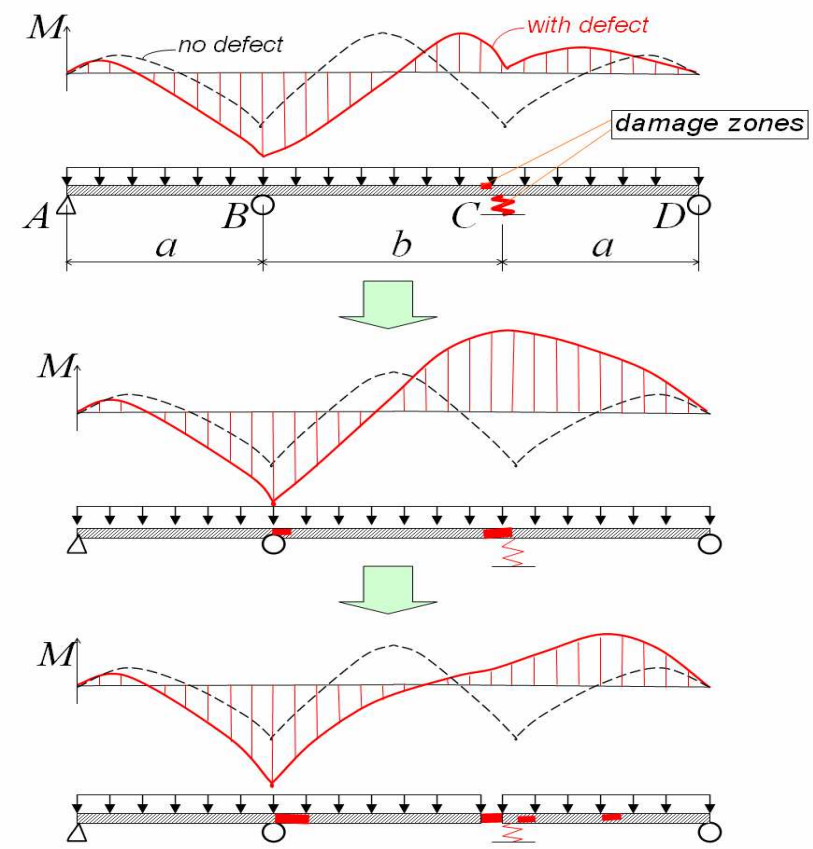

Fig. 13 The defect evolution at the pin-point C causes redistribution of bending moment (red solid line), which triggers the damages at other locations and final structural failure

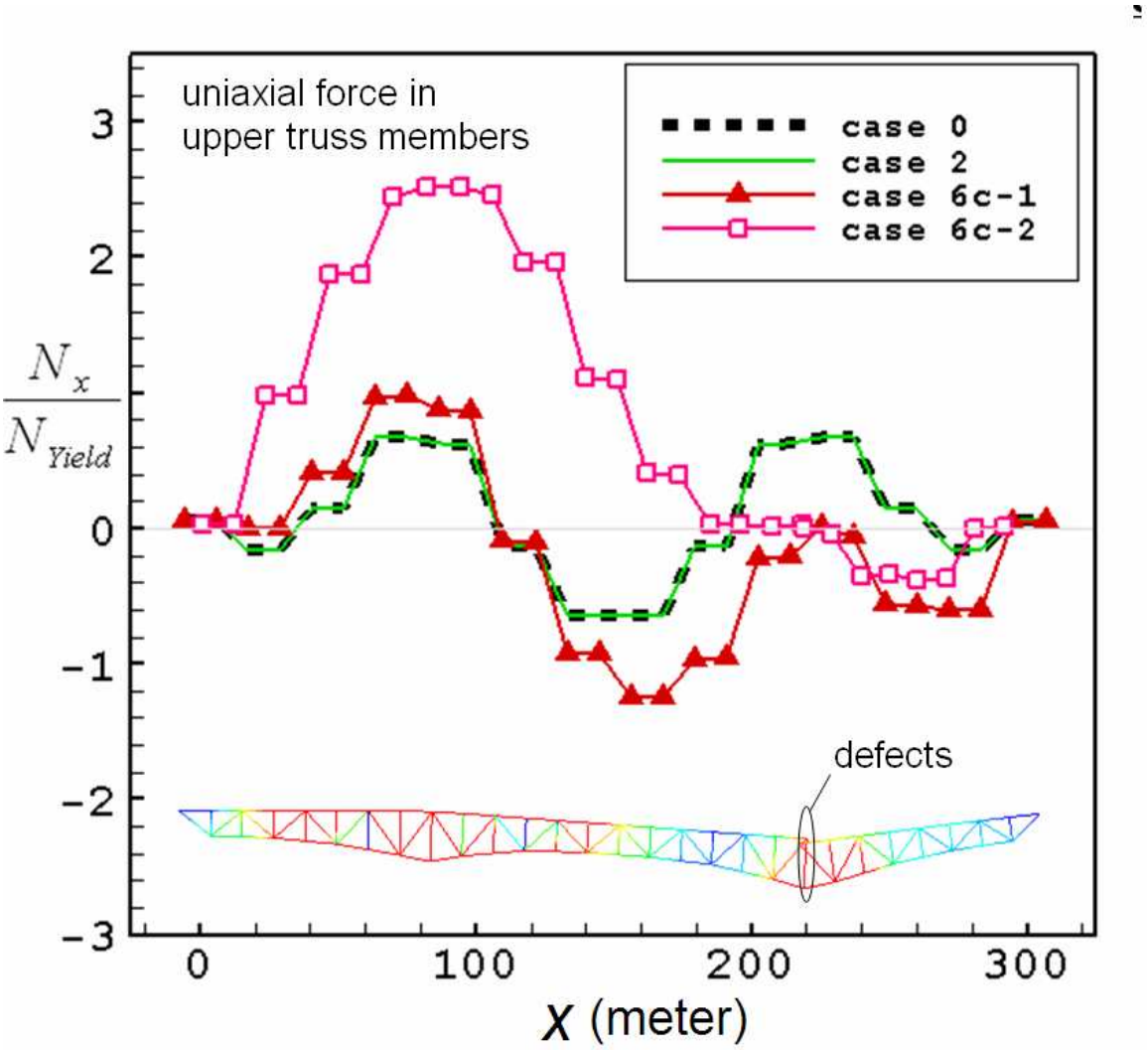

Fig. 14 The uniaxial force distribution in upper truss members, a comparison between the cases of defect-free and the case 6c-1,2 – the defects modeled by cohesive law with two different softening rate.

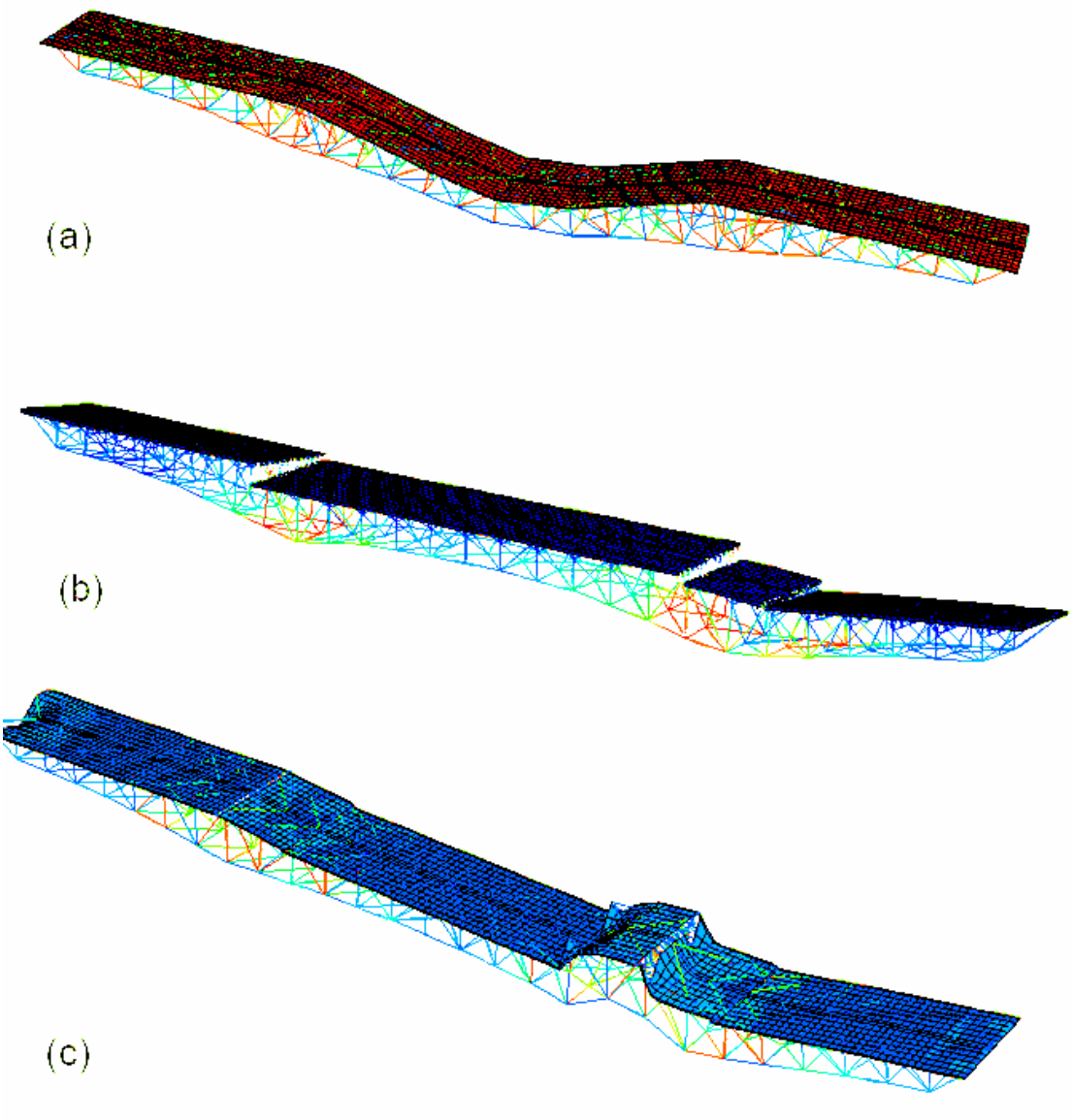

Fig. 15 Three patterns of material's failure-induced structural failure

4.3 Identification of the Initial Spot(s) of the Fracture and the Failure Process*

Fig.15 present three patterns of the defect (material's failure) induced structural failure. Phenomenonlogically, the one in Fig. 15c is most close to the observed debris

* **This section identifies that the failure started at the south end around the pier. Fig. 16 is taken as the evidence for this conclusion; which essentially matches the NSTB's findings because of the heavy surface load there. However, due to imperfacted information the author could have at the time, in the text the "pier 5" has been written as "pier 7"; also the prime attached to a node's symble should be reversed, i.e. U'_{9E} should be U_{9E} and verse visa, according to NTSB's convention. These minos confusions have no effect on the obtained conclusions. (noted by Su Hao at May 14, 2008)**

distributions. In this simulation the severe defect was pre-assigned to the area around U'_{9E} and a less severe defect was to L'_{8E}; these defects are assumed to be existing cracks. Also moderate cohesive elements have been implemented at the areas around $U'_{7E}U'_{7W}$ and $U_{8E}U_{8W}$ to promote the formation of plastic hinge.

According to the numerical simulation, the evolution of the pattern in Fig. 15c can be described as the sequence as follows: (1) the defect at U'_{9E} propagates rapidly to U'_{9W} and cuts the upper deck; (2) the load on the south pilot span pulls the truss members above pier 7 towards south which promotes the defect growth at L'_{8E}; (3) plastic hinges and subsequent fracture occur around both the north end of main span ($U_{8E}U_{8W}$) and the south pilot span ($U'_{7E}U'_{7W}$); (4) large strain concentrations, which represents the secondary plastic hinges, appear in low level truss members near $L'_{8E}L'_{8W}$ and $L_{8E}L_{8W}$; it accelerates the collapse of the main and south spans.

Hence, based on the analysis and simulation carried out in this report, the preliminary conclusion is that the fatigue-induced defects do exist before the accident. The most suspicious locations of the defects are the upper main truss joint above the pier 7 east and the joint of lower main truss members near the fixed pin-point of pier 7 east. The material-failure around these locations causes subsequent structural failure that leads to the collapse of the bridge.

4.4 Further Questions

Another two unsolved issues among many more:

(I) how to ensure that the material's failure starts at the south end of main span?

(II) where is the exact location of the initial defect around $U'_{9E}U'_{9W}U'_{8E}U'_{8W}$?

Regarding (I): according the analysis of case 0 and case 2, it has been found that no essential difference between north and south in stress and moment distributions in critical locations. However, the photographic picture of the north end collapse captured by the video recorder at south end (Fig. 16) shows a slight slope of the main body when it fell into water, which is an evident that the south side collapse came first, provides no significant deformation associated with the plastic hinge at the central point of the bridge.

Regarding (II), due to lack of the detail information about the concrete deck and its connection to upper truss members, the performed analysis is not enough to draw conclusion about this part.

Fig. 16 The instance that main span fell into water

4.7 An Example of Historical Disaster: Ludendorf Bridge

The collapse of Ludendorf bridge on Reihn River of West Germany at 1945 winter may provide some hints for the current analysis. The three-span truss bridge (Fig. 17a) was built at 1919 just after World War I with classical upper-truss design, so the road deck is in the bottom where the peak moment-induced tension presents. It had been captured peacefully by U. S. Army at the beginning of 1945 and 6 large army units passed safely. But then it collapsed without live-load presented. Due to the strategic importance the bridge was heavily guarded by G.I., which excludes the possibility of Nazi's action. According to the photopicture(Fig. 17b) it looks like the middle part initiated the failure. It is speculated that the passed heavy army equipments accelerated the fatigue propagation of some existing defects, the localized material's failure caused the following structural failure since no active load when the accident occurs. Ten years ago the author of this report visited the ruins of the bridge. Now there is a status to symbol the corporation between U. S. and West Germany Arms in Nato.

(a) The three-pan upper trussed bridge on the Reihn, Western Germany; built at 1919 after the name of General Ludendorf of Deutch Army

(b) the wrecks of the bridge after it collapsed at 1945

Fig. 17 Historic example: the collapse of Ludendorf bridge of Reihn at 1945 (photopictures collected from the documentary "Definitive history of WWII, published by Brentwood L.L.C. and de.wikipedia.org)

5 Suggestions

The analysis in the previous sections concludes the existence of fatigue-induced defect before the accident. A more important task is probably to find the reasons that hamper us to have presentiments of the hiding risk that the bridge 9340 had. In order to avoid the similar tragedy happens again in the similar structured bridges on operation,

Based on the analysis and computations carried out and public available information, this report suggests a "hybrid bridge living-monitor system" to the veteran bridges that are suspected with defects and still under operation. This system including four parts: daily stress measurement and monitor by permanently-attached strain gauges (or other effective measurement methods) at key spots, regular inspection with shortened time interval and additional attentions to the key locations; thoroughly finite element analysis of the entire bridge structure including details of truss-joints; and the analysis of the existing risk based on the standard and the integrated information from both measurement and computations. This system should be able to provide dynamic information of the bridge so to assist the corresponding administration make necessary decision on time. To make the system to be effective, this report suggests the attentions to the following three issues

- Bending moment in truss member and associated stress concentration: Accurate computation of the stress concentration around truss-joint is the prerequisite to obtain correct estimate of fatigue life. Due to the limited computation capability in past, it seems that the original design and subsequent early investigations could only treat the 9340 bridge as a truss-assembled structure, which led to the focus onto the forces and damage conditions in truss members. Although this is a commonly accepted engineering approach, in many cases it may underestimate the risk of fatigue-induced defect since it underestimates the bending moment induced stress in general, especially at truss-joints when rust-induced fixed-pin effect and thermal induced constraint become significant.
- The effect of stress superposition: strain gauges is an effective tool to capture and monitor "*in situ*" stresses on an engineering structure; however, it is limited to measure the change of stress after it is attached to the structure, for example, the difference of live loads between rush hours and that at midnight. A pre-existing stress state, such as residual stress and dead load (weight) induced stresses, can not be detected by strain gauge except it has been attached before the assembling of the bridge. Hence, merely strain gauge measurement [2] is usually insufficient to obtain the actual stress amplitude. An on site measurement in conjunction with computation is an efficient and accurate way to monitor stresses in an engineering structure, which is the central of the proposed "hybrid living-monitor system".
- Fatigue life estimate: The Miner's law is a recommended formula for estimate of the fatigue life of steel bridge; but it may underestimate the risk of the cases with existing macro-scale defect. This is because a fatigue-induced failure of steel components can be approximately divided into three stages: damages

accumulation-induced macro-scale crack initiation, fatigue crack growth, and fast propagation with subsequent material's failure. Miner's law is originally developed to describe the first stage. The evolution speed of defect such as a crack growth is generally accelerated in the second stage when applied load remains. Paris' law is relatively accurate under this situation.

Also, regarding the ongoing investigation, this report suggests the following measurements:

- Preserve all broken sections, especially these near the pier-supports of the main span; the corresponding fractographic analysis may distinguish defects from different "ages". For example, a crack could be created before and during bridge component manufacturing and assembling, or was promoted by the fatigue loads in past 40 years, or occurred by ductile tearing and fast brittle crack propagation during the collapse, or is just the damages caused by the impact of fallen concrete deck.
- Perform microscale graphic analysis, such as TEM and SEM at certain positions; which may help to identify the deformation stage of the material and the stress level during the accident, which can be used to ascertain the occurrences of plastic hinges so as to verify computed failure model.
- Perform mechanical properties measurements by the specimens cut from failed component at key-positions, e.g. welded joint, heat effective zone, and steel matrix. These measurements include at least uniaxial tension, fracture toughness test and two classes of fatigue tests, i.e. the notched rotation bar test to measure the parameters in Miner's law and the fatigue crack propagation test in fracture mechanics specimen to measure the parameters of Paris' law.

The fundamental information provided by these suggested measurements will not only be useful to the current investigation, it could also be vital important for the safety evaluation of other similar-structured bridges under operation.

Publicly Disclosed Inspection Report and Fatigue Life Analyses

[1] Draft Report: Fatigue Evaluation and Redundancy Analysis, Bridge No. 9340, URC Corporation, 2006
[2] Fatigue Evaluation of the Deck Truss of Bridge 9340, University of Minnesota, 2001

